2011

Comprehensive model of oxygen steelmaking part 2: application of bloated droplet theory for decarburization in emulsion zone

Neslihan Dogan
University of Wollongong, ndogan@uow.edu.au

Geoffrey A. Brooks
Swinburne University of Technology

Akbar Rhamdhani
Swinburne University

Publication Details

Dogan, N., Brooks, G. A. & Rhamdhani, A. (2011). Comprehensive model of oxygen steelmaking part 2: application of bloated droplet theory for decarburization in emulsion zone. ISIJ International, 51 (7), 1093-1101.

ISIJ International, Vol. 51 (2011), No. 7, pp. 1093–1101

Comprehensive Model of Oxygen Steelmaking Part 2: Application of Bloated Droplet Theory for Decarburization in Emulsion Zone

Neslihan DOGAN, Geoffrey Alan BROOKS and Muhammad Akbar RHAMDHANI

Faculty of Engineering and Industrial Science, Swinburne University of Technology, Hawthorn, VIC 3122 Australia.
Email: doganeslihan@gmail.com

(*Received on February 8, 2011; accepted on April 20, 2011*)

The development of a global model for oxygen steelmaking and its validation against industrial data was reported in Part 1 of this paper. This paper focused on the development of one sub-model on the decarburization reaction in the emulsion zone incorporating the bloated droplet theory. This paper also critically evaluated the current knowledge on the kinetics of decarburization reaction in the emulsion phase and discussed the repercussions of the new model for industrial practices. The decarburization model, in conjunction with the industrial data, indicates that the decarburization rates in the emulsion phase reaches up to approximately 60% of the overall decarburization rate during the main blow. It was found that the residence time of droplets as well as decarburization reaction rate via emulsified droplets was strong function of bloating behavior of metal droplets in the emulsion phase. The estimated residence times of the metal droplets in the emulsion were between 0.4 to 45 s throughout the blow. The influence of variations in droplet size and ejection angle on residence time and decarburization rates via emulsified droplets was also investigated. It was shown in this study that the decarburization rates in the emulsion were accelerated if droplet size was decreased or if the ejection angle was decreased.

KEY WORDS: bloating; droplet size; droplet angle; residence time of droplets; decarburization; oxygen steelmaking.

1. Introduction

An improved understanding of decarburization reaction and the factors controlling the overall rate should provide better control of the process and increase the productivity. In the literature, there is a limited knowledge on how to relate the carbon removal rate within the droplets to the overall kinetics of the process under full scale operating conditions.

A computer based model which incorporates the bloated droplet theory under dynamic conditions was developed. The process variables influencing the decarburization kinetics considered in the model were hot metal, scrap and flux charges, hot metal, scrap and slag compositions, oxygen blowing conditions such as lance height, gas flow rates, temperature of the bath, flux dissolution, scrap melting, ejected metal droplets behavior such as droplet generation rate, droplet size, residence time in the emulsion and decarburization rates in the emulsion and impact zones. All selected process variables were modelled individually in which they include the calculation procedure, assumptions and boundary conditions to represent each process variable considered. The developed sub-models were applied into the industrial data, reported in the literature, for verification and validation purposes. In the following step, the sub models were linked to each other dynamically to be used as input data or boundary condition and sub-models formed the global model of the oxygen steelmaking process. Finally, the results of the proposed global model were compared with a full set of industrial data to investigate the feasibility of the application of the developed model. The model development and validation are discussed in Part 1 of this paper. In Part 2 of this paper, the development of one sub-model in the global model, *i.e.* the decarburization reaction in the emulsion phase incorporating a bloated droplet theory and a droplet residence model will be discussed.

1.1. Bloated Droplet Theory

It is generally accepted that the decarburization reaction in the emulsion phase takes place via FeO reduction. On the basis of x-ray transmission photographs[1–4] and the analysis of the experimental results,[3–5] it is believed that the reaction takes place in two steps via bubble formation. As the metal droplets are ejected from the liquid metal, they react with FeO in slag. FeO diffuses to the slag-gas interface towards a bubble sitting on the metal-gas interface to supply oxygen. CO reduces FeO at slag-gas interface and followed by reaction at the metal-gas interface with CO_2 diffusion through a gas halo.[4] CO_2 provides oxygen to react with carbon in the melt. These reactions involve the sequence[4]

$$CO_{(g)} + (FeO) = Fe + CO_{2(g)} \quad \text{(slag surface)} \ldots\ldots (1)$$

$$CO_{2(g)} + [C] = 2CO_{(g)} \text{ (metal surface)} \quad \text{..... (2)}$$

The overall reaction is

$$(FeO) + [C] = Fe + CO_{(g)} \quad \text{..... (3)}$$

These sequential reactions continue until the bubble leaves the slag-metal interface. Accordingly, carbon content of metal droplets will decrease and numerous CO gas bubbles will be formed. The reaction product, CO gas provides stirring to the emulsion phase. It is believed that the decarburization reaction via FeO reduction is responsible for the majority of decarburization in oxygen steelmaking process and this reaction is also important to slag foaming and sloping during the process.

There is evidence that a CO gas halo formation surrounds metal droplet when iron droplets containing high carbon content (up to 4 mass%) reacts with an oxygen steelmaking slag. Mulholland *et al*.[1] first observed the gas halo surrounding Fe–C–S droplets in slag using x-ray fluoroscopy technique. Other researchers[3,4,6–9] provided further evidence of the formation of gas halo. This phenomenon may occur due to high rate of external nucleation of CO gas compared to the internal nucleation. In such case, the energy barrier for nucleation is reduced due to the sufficient amount of C and O available at slag-metal interface, which is called external nucleation.[6] When oxygen diffuses through a droplet, CO pressure increases with time. And if CO pressure exceeds the ambient pressure, the metal droplet become supersaturated and the reaction of oxygen and carbon becomes possible.[10]

When internal pressure of CO exceeds the surface energy of the metal droplet, CO gas formation occurs inside metal droplet.[11] CO gas pressure depends on the carbon and oxygen concentration, temperature and concentration of other impurities inside the metal droplet. The build up rate of bulk oxygen depends on the difference between the oxygen absorption rate and rate of consumption of this oxygen at the surface due to the decarburization and iron oxide formation.[11]

As the internal nucleation started, metal droplet becomes "bloated" and surface area increases therefore reaction kinetics increases since the turbulence caused by the generation of CO bubbles inside the metal droplet promotes the diffusivities.[12] The bloating behavior of metal droplets is suggested due to the generation of CO bubbles inside the metal droplet.[7,10,13] Please note, some researchers use the term "swelling" instead of "bloating" in the literature.

Baker *et al*.[14–16] first observed the metal droplet exploded due to the CO nucleation inside the metal droplet when passing through a gas mixture of oxygen and helium. The similar observations have been done by Sun and his coworkers.[17] They found that the supply rate of oxygen from the bulk gas is faster than the oxygen consumption rate at the surface by the reaction. Later, Sun and his coworkers[10,12] studied the bloating behavior of iron droplets in oxidizing slags and they investigated the effects of composition of metal droplet on the reaction rate of decarburization in oxidizing slag. They found that decarburization rate was retarded due to the other oxidation reactions in the metal droplets. The kinetic model results for decarburization rate agreed with those of their experimental observations and Molloseau and Fruehan's experimental study at low FeO content (<5 mass%). However, the decarburization rate predicted by Sun *et al*.[10] was underestimated when FeO content is higher than 10%. They stated disagreement might be due to the bloating behavior of droplets since they did not include the increase in interfacial area and the contribution of reactions inside the metal droplets. They found that there is an incubation period for bloating phenomena and they suggested that some time is required to build up the oversaturation level for CO nucleation within the droplet. They concluded that CO nucleation within the droplet is responsible for the bloating of droplets.

Min and Fruehan[4] carried out an experimental study to measure the decarburization rate of droplet in steelmaking slags containing low FeO content. Molloseau and Fruehan[3] further studied this phenomenon for slags containing between 3 and 35 mass% FeO. This study is the first study investigating the behavior of dense and bloated droplets under various FeO concentrations. They measured that the reaction rate of bloated droplets was one to two orders of magnitude faster than the rates for dense droplets. Based on their observations, they suggested that FeO transfer in the slag is the possible rate limiting step for decarburization rate of bloated droplets whereas the reaction rate of dense droplets is controlled by dissociation of CO_2 on the metal.

Chen and Coley[7,13] conducted an experimental study to predict the nucleation rate of CO inside the metal droplets using x-ray fluoroscopy technique at various temperatures. They found that the diameter of droplets increased to 1.5 times the original. This observation is in good agreement with those reported by Molloseau and Fruehan.[3] The gas generation rate is suggested to be controlled by the rate of nucleation of CO gas bubbles inside the droplet due to the dependency of the reaction rate on the droplet size.

The current observations showed that metal droplets are "bloated" with CO gas, generated during the active decarburization period when FeO concentration in the slag is higher than 10 mass% in the emulsion phase. The droplets become less dense and suspended longer time in the emulsion. Alternatively, if the rate of carbon removal is weak, the reaction product, CO gas escapes easily and detaches from the droplet as a result, droplet maintains its original shape.[3] These studies indicated that droplet emulsification has crucial factor on decarburization kinetics of oxygen steelmaking process.

2. Model Development

The theoretical treatment suggested by Brooks *et al*.[18] is applied in this study to estimate the decarburization rates of metal droplets as a function of the dynamic changes in droplets behavior. Using this approach, total decarburization rate in the emulsion zone can be obtained from the summation of decarburization rates of individual metal droplets as a function of droplets volume due to the bloating behavior of droplets. In the model, the metal droplets are ejected with rate, R_B to the slag phase, generated droplets, whose residence time is smaller than given time-step, return from the emulsion zone with rate R_D. When the steady state conditions reach, the droplet generation rate will be equal to the droplet returning rate. The droplet generation rate can be

obtained using blowing number as proposed by Subagyo and Brooks.[19] The rate of metal droplets returning to the metal bath with respect to residence time, *tr* can be written as;

$$R_{Di} = \begin{cases} 0 & \Delta t < tr_{ij} \\ R_{Bi} & \Delta t \geq tr_{ij} \end{cases} \quad \text{..... (4)}$$

Here *i* represents the ejected time of metal droplets and *j* represents the blowing time of the process. Since all the droplets ejected at each time step are assumed to have the same residence time for a defined droplet size, the mass of metal droplets in the emulsion with respect to residence time, *tr* can be written as;

$$V_{Bi} = \begin{cases} R_{Bi}\Delta t & \Delta t < tr_{ij} \\ R_{Bi} tr_{ij} & \Delta t \geq tr_{ij} \end{cases} \quad \text{..... (5)}$$

The mass of metal droplets returning is the remaining mass of metal droplets generated after decarburization reaction. It can be calculated by substitution of the quantity of carbon removed from the quantity of metal droplets ejected at time *i*. The relationship is given as;

$$V_{Di} = \begin{cases} 0 & \Delta t < tr_{ij} \\ R_{Bi}\Delta t - \dfrac{m_i\left(C_i^{t+\Delta t} - C_i^t\right)}{100} & \Delta t \geq tr_{ij} \end{cases} \quad \text{.... (6)}$$

where m_i is the weight of a single droplet (kg). Thus, the decarburization rate can be calculated using;

$$\frac{dW_C}{dt} = \frac{\sum_{i=1}^{m} \frac{m_i}{100}\left(C_i^{t+\Delta t} - C_i^t\right)}{\Delta t} \quad \text{..... (7)}$$

2.1. Droplet Residence Model

This model is designed to calculate the residence time of metal droplets ejected to the emulsion phase as a function of physical properties of slag, FeO concentration of slag, carbon concentration of metal and droplet generation due to the jet intensity.

The model developed by Brooks *et al*.[20] has been applied in this study since it includes the dynamics of the motion of droplets in the slag-gas-metal emulsion phase. In the proposed model, force balance was made based on the ballistic motion of a single droplet at vertical and horizontal coordinates. The motion of a single droplet is illustrated in **Fig. 1**. The relationship between the forces can be represented for horizontal and vertical coordinates in the following equations.[20]

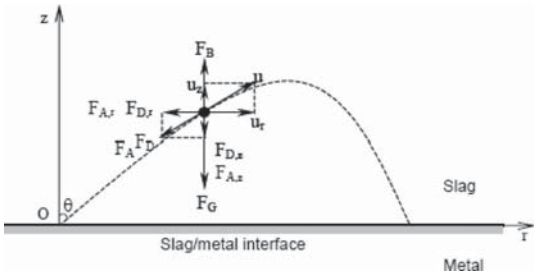

Fig. 1. The schematic illustration of ballistic motion of a metal droplet in slag.[20]

for z direction:

$$\rho_d V_d \frac{du_z}{dt} = F_B - F_G - F_{D,z} - F_{A,z} \quad \text{..... (8)}$$

for r direction:

$$\rho_d V_d \frac{du_r}{dt} = -F_{D,r} - F_{A,r} \quad \text{..... (9)}$$

where u_z and u_r are the velocity of droplet for *z* and *r* directions, respectively. Variables ρ_d and V_d refer to density and volume of droplet. F_B, F_G, F_D and F_A are buoyancy, gravitation, drag and added mass forces, respectively.[20] Further assuming the droplet is spherical in shape with diameter D_d and introducing definitions of the relevant forces in terms of density, velocity and diameter of the droplet, by mathematical derivation, we can obtain the following differential equations that govern the motion of the droplet in the slag:

$$\frac{du_z}{dt} = \frac{2(\rho_s - \rho_d)g}{\rho_s + 2\rho_d} - \frac{\rho_s C_{D,z}}{\rho_s + 2\rho_d} \cdot \frac{A_{d,p}}{V_d} u_z^2 \quad \text{..... (10)}$$

$$\frac{du_r}{dt} = -\frac{\rho_s C_{D,r}}{\rho_s + 2\rho_d} \cdot \frac{A_{dp}}{V_d} u_r^2 \quad \text{.....(11)}$$

Equations (10) and (11) are the major differential equations to be solved, based on which a mathematical model for predicting the trajectory and residence time of a metal droplet moving in slag is developed. The details of the model development can be found in an earlier article by the authors.[20]

This model is called "ballistic motion model" and is valid for dense droplets. The dense droplets can be seen under the conditions of weak decarburization rates. In order to calculate the residence time of bloated droplets, threshold decarburization rate should be calculated. The bloating behavior phenomenon cannot yet be completely explained from basic principles, so empiricism was introduced. As a consequence, threshold decarburization rate was evaluated from the experimental study by Molloseau and Fruehan[3] and calculated as a function of FeO content in the slag using;[20]

$$r_c^* = 2.86\times10^{-4}\left(\text{mass\%FeO}\right) \quad \text{..... (12)}$$

Subsequently, the apparent density of droplet can be calculated as a function of initial density and the rate of decarburization reaction given by;[20]

$$\rho_d = \rho_{d0}\frac{r_c^*}{r_c} \quad \text{..... (13)}$$

where ρ_{d0} is the initial density of a droplet, r_c is the decarburization rate and r_c^* is the threshold decarburization rate. If there is no bloating motion of droplet, the apparent density of droplet is equivalent to its initial density. It is represented as;[20]

$$\rho_d = \rho_{d0} \quad \text{..... (14)}$$

2.2. Rate-Determining Step

In this model, the reactions shown in Eqs. (1)–(2) are not considered and "halo" phenomenon as observed by some researchers[1,3,4,6–9] was not taken into account. Only Eq. (3)

was included for the calculation of the decarburization rate of the metal droplets in the emulsion phase. The kinetic model proposed by Brooks *et al*.,[18] based on a simple surface renewal model of carbon diffusions, was applied in this study. The selection of this model can be found in an earlier article by the authors.[20] It is important to note that the Brooks *et al*. model used empirical data from the Molloseau and Fruehan study for some of their parameters in their model, so in effect, "fitted" their model to the data, and they only claimed that this model is useful for global kinetic calculations and not necessarily the "correct" kinetic model. The carbon diffusion with the metal droplets might be the rate controlling step for the bloated droplets since there is sufficient oxygen available in the system so that CO gas generation rate is high and metal droplets become bloated. The gas halo formation observed by some researchers[1,3,4,6–9] may be important to understand the mechanism of the reactions between droplets and slag in the emulsion but was not taken into account in our model. Our model using the data from Molloseau and Fruehan,[3] focussed on connecting "bloating behaviour of the droplets with their residence time in the emulsion with the overall decarburization kinetics. Nevertheless, further work is required to fully understand the reaction mechanism at the individual droplet level.[20] The approach of Brooks *et al*. has been successfully applied to the experimental results[3] and we have incorporated this approach into our global model.

Other impurities such as silicon and manganese have an impact on the decarburization rates of metal droplets in the oxidizing slag. It should be noted that only the model developed by Sun and Zhang[12] considered the metal droplets containing low silicon and manganese content (below 1 mass%). In their work, it was predicted that decarburization reaction rate was also suppressed and the effect of impurities was lower. However, these predictions were not validated against an experimental or industrial data. In conclusion, other impurities have a potential to decrease the decarburization rates of metal droplets in the slag. Particularly, high silicon could cause the formation of SiO_2 at the start of the blow that retards decarburization reaction. There is very limited data available in the literature on the effect of impurities on decarburization. Additionally, the industrial data used in this study has no information about the impurities within the metal droplets. For simplicity, it was assumed that droplets only contain carbon and the effects of other impurities were not included.

2.3. Basis of the Model

The following assumptions have been made in the model based on the industrial data available for a 200-ton oxygen steelmaking furnace. The operational conditions used for these calculations were taken from the industrial data reported by Cicutti *et al*.[21,22] and are given in **Table 1**. **Figure 2** shows the variation in lance height and inert gas flow rate with sampling points for metal and gas phase. The outcome of other refining reactions such as FeO concentration was entered as known variables.

1) It is known that the carbon content of metal droplet ejected from the bath is lower than carbon content of the liquid metal. However, there is no calculation technique available to predict the initial carbon concentration of metal droplets. Therefore, it was assumed that carbon content of the metal droplet was equal to the bulk carbon content of the liquid metal. Bulk carbon content was calculated using mass balance, which includes scrap melting, the decarburization reaction in the emulsion zone.

Table 1. Data for numerical calculation.

Hot metal charged	170 000 kg
Scrap charged	30 000 kg
Oxygen flow rate	620 Nm^3/min
Supply pressure	10^6 Pa
Number of nozzle	6
Throat diameter of nozzle	0.033 m
Exit diameter of nozzle	0.045 m
Inclination angle	17.5°
Lance height	1.8–2.5 m
Initial hot metal temperature	1 623 K
Tapping temperature	1 923 K

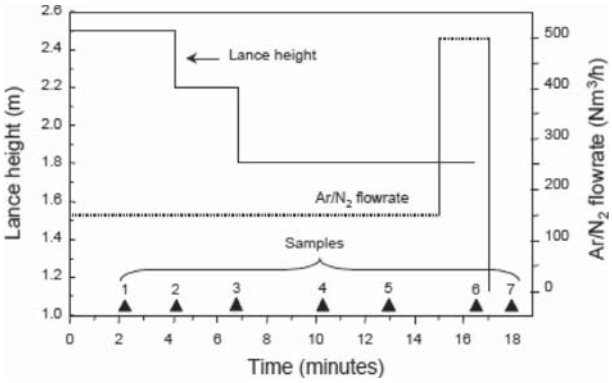

Fig. 2. The variation in lance height, inert gas flow rate and sampling point during the blowing process.

The value of initial carbon content of metal droplets generated was fed as an input data to the Droplet Residence (RD) Model (described in more details in the Part 1 paper). With regard to the residence time, the difference in carbon concentration was obtained from RD Model. The generated droplets, whose residence time is smaller than defined time-step, are returning from the emulsion phase. If the residence time was larger than the time-step, decarburization of droplets with that particular residence time was added to calculate the rate of overall decarburization in the emulsion phase as per Eq. (7).

2) In this model, effective mass transfer coefficient, k_{eff} was calculated on the basis of Higbie's penetration theory.[23] This theory was employed by Brooks *et al*.[20] to predict the mass transfer coefficient of carbon to the interface based on the residence time of the dense and bloated droplets. The relationship is;

$$k_{eff} = 2\sqrt{\frac{D_C u_d}{\pi D_p}} \quad \text{..... (15)}$$

where D_C is the diffusivity of carbon and u_d is the overall velocity of droplet.

3) The effect of size distribution was not included and the

diameter of a metal droplet was assumed to be 2 mm since the mean value ranges from 1 to 2 mm reported by Price *et al*.[24] And this value is valid for the industrial data taken from Cicutti *et al*. They also stated that drop size varies from 0.23 mm to 3.35 mm.[22]

4) Subagyo *et al*.[20,25] proposed that the ejection angle of bloated droplets is a minor effect on the residence time calculations since the motion of the droplets is dominated by buoyancy. In this study, the effect of ejection angle was evaluated.

5) Diffusivity of carbon in liquid iron is 2×10^{-9} m^2/s at 1 600°C.[26] Diffusivity of carbon will then be determined as a function of slag temperature and viscosity of slag-metal-gas emulsion based on the Stokes-Einstein and Eyring equations for various temperatures. It was assumed that slag temperature increases linearly and was 100°C higher than bath temperature.

6) For a slag-metal-gas emulsion, the motion of metal droplets is influenced by the gas bubbles trapped in the gas phase. The metal droplets are treated as dispersed phase in a slag-gas continuum. The average density and viscosity of the slag-gas continuum was calculated by the following equations.[20,27]

$$\rho_{sg} = \rho_g \varphi_g + \rho_s \left(1-\varphi_g\right) \quad \text{..... (16)}$$

$$\mu_{sg} = \frac{2}{3}\frac{\mu_s}{\left(1-\varphi_g^{1/3}\right)}\frac{\left(\rho_{sg}-\rho_g\right)}{\left(\rho_s-\rho_g\right)} \quad \text{..... (17)}$$

Here ϕ_g refers to the volume fraction of the gas in the emulsion and can be given by;[20]

$$\phi_g = \frac{V_s}{V_g + V_m + V_s} \quad \text{..... (18)}$$

Initially, the density and viscosity of slag was calculated as a function of slag composition and temperature. These values were entered as an input data in the droplet residence model. The average density and viscosity of slag-gas continuum were calculated as a function of gas volume, as given in Eqs. (10) and (11) to predict the velocity of the droplets at z and r directions.

7) The initial velocity of a droplet was estimated based on the conservation of energy relationship proposed by Subagyo *et al*.[25] The relationship suggests that the kinetic energy of blown gas is used to generate and eject the droplets. The kinetic energy absorbed by a metal droplet from oxygen jet, E_{Kd} is calculated using;[25]

$$E_{Kd} = \frac{1}{2} R_B u_{d(0)}^2 \quad \text{..... (19)}$$

where R_B and $u_{d(0)}$ denote droplet generation rate and initial velocity of droplets, respectively. This relationship is valid if the all produced droplets are in spherical shape. The kinetic energy of the blowing gas E_{Kg}, is;[25]

$$E_{Kg} = \frac{1}{2} \rho_g R_G u_g^2 \quad \text{..... (20)}$$

The kinetic energy absorbed by the metal droplets was correlated to kinetic energy of blown gas as a function of blowing number, N_B based on the experimental data reported by Subagyo *et al*.[25] and Koria and Lange.[28] The correlation is given in the following[25]

$$\frac{E_{Kd}}{E_{Kg}} = 0.00143 N_B^{0.7} \quad \text{..... (21)}$$

8) The equilibrium concentrations of carbon and iron oxide were determined by the activity coefficient and concentration. The activity of carbon follows Henry's Law and was calculated from the interaction parameter of carbon itself since it was assumed that carbon is the only substitute in the metal droplet.[29] Alternatively, Raultian activity coefficient of iron oxide was determined as a function of temperature and composition of other oxides in slag. The data for activity coefficients were taken from the literature.[30,31]

9) The apparent surface area and volume of the droplet varied as a function of the droplet density and mass. Firstly, the droplet density was calculated using Eq. (14) and droplet mass decreases as the carbon was removed from the droplet. These values were entered into the following equations.

$$V_{app} = \frac{m}{\rho_d} \quad \text{..... (22)}$$

$$D_p = \sqrt[3]{\frac{6V_{app}}{\pi}} \quad \text{..... (23)}$$

$$A_{app} = \frac{1}{4}\pi D_p^2 \quad \text{..... (24)}$$

10) Ito and Fruehan[32,33] reported that gas fraction in the slag-metal-gas emulsion varies between 0.7 and 0.9. Average value of this range, 0.8 was used in the calculations of slag-gas continuum in this study.

11) Slag foam height was assumed to be constant and it was equal to 2 m. In oxygen steelmaking furnace, the foam height might reach to the mouth of the furnace, particularly during the main blowing period. An assessment of this assumption will be discussed in the results section.

2.4. Formulation of the Model

The blowing conditions, such as variation in lance height and presumed slag composition were entered as input data to the RD sub-model. The slag properties were calculated as a function of slag composition and temperature. The calculation procedure of physical properties of slag was provided in the previous publication.[34] Droplet generation was then calculated as a function of blowing conditions as explained elsewhere.[35] The output results of droplet generation sub-model were used to calculate the initial velocity of metal droplets ejected to the emulsion phase and to calculate the quantity of metal droplets ejected. Then, the velocity and trajectory of metal droplets were obtained based on the finite difference technique. The values of droplet velocity as a function of change in droplet diameter were put into to Eq. (15) to calculate the effective mass transfer coefficient. Therefore, the decarburization rate in the metal droplets and the change in the carbon concentration of metal droplets can be calculated. If the decarburization rate is higher than threshold decarburization, bloating occurs. This calculation procedure was repeated until the trajectory of metal droplets at z direction reaches to zero. The time step was selected based on previous work by Brooks *et al*.,[20] that demonstrated that below time steps below millisecond was required to

ensure that the predictions did not significantly differ with different time steps. Accordingly, 0.0001 s was selected which is sufficient enough for the numerical accuracy and for computational time. The output values for residence time and the change in carbon content of metal droplets were taken from droplet residence sub-model to feed into the decarburization in emulsion sub-model as an input data. Based on the droplet residence, the quantity of metal droplets in the emulsion phase and the quantity of metal droplets returning to the metal bath were calculated using Eqs. (5) and (6), respectively. And the total decarburization rate within the individual droplets was calculated using Eq. (7).

3. Results and Discussion

3.1. Droplet Residence

Figure 3 illustrates the evolution of residence time of droplets with a diameter of 2 mm as a function of carbon concentration in the bath as predicted by the proposed model. In the early part of the blow, the residence time of droplets is around 45 s. Towards the end of the blow, it decreases to 0.4 s. As seen, the residence time of droplets is much higher in the presence of high carbon concentrations. Towards the end of the blow, the residence time is low due to the weak decarburization rates. This may imply that metal droplets are "bloated" with CO gas, generated during the active decarburization period, become less dense and spend longer time in the emulsion.[4] However, towards the end of the blow, the metal droplets maintain their original density due to the slow decarburization. As a result, it has been concluded that decarburization rate is strongly dependent on the residence time of droplets in the emulsion and that the bloating of droplet is critical to understand the overall kinetics of steelmaking. It was found that running the model without the bloated droplet included (every droplet is dense) results in a vastly under predicted overall decarburization rate.

Further simulations were performed to investigate the change in residence time as a function of droplet size. **Figure 4** compares the residence time of metal-droplets in the emulsion over a range of sizes in relation to the ejection time. It is evident that the residence time of droplets with high carbon content is higher with regardless to the initial droplet size owing to spontaneous CO formation in the early blow. Furthermore, droplets except the ones with diameter of 3 mm have same pattern. Their residence time decrease and increase slightly approximately at the 9 min after the start of the blow and followed by a sharp decrease towards the end of the blow. The larger droplets with low carbon concentrations do not become bloated and returned to the bath simultaneously.

Significant differences in droplet residence time are also due to the physical properties of slag as a function of gas volume fraction. For example, gas hold up of 80% in the emulsion increases the viscosity of slag-gas continuum two times the viscosity of slag and it decreases the density of slag-gas continuum four times the density of slag. The effects of gas hold-up will be a subject of a future publication. However it should be noted that carbon content of liquid iron has a predominant role on the residence time of droplets.

3.2. Decarburization Rates in Emulsion Zone

The proportion of decarburization via emulsion as a function of bulk carbon content is given in **Fig. 5**. The overall decarburization rate was obtained by the summation of instantaneous decarburization rates from emulsion and impact zones. The refining rate in emulsion zone decreases as the carbon content of the metal decreases. However, there

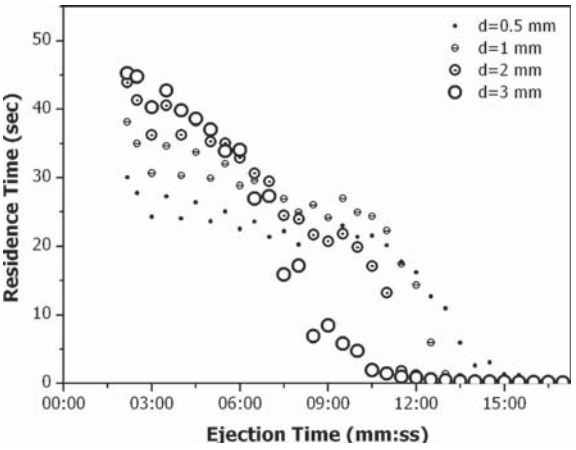

Fig. 4. Variations in residence time as a function of initial droplet size.

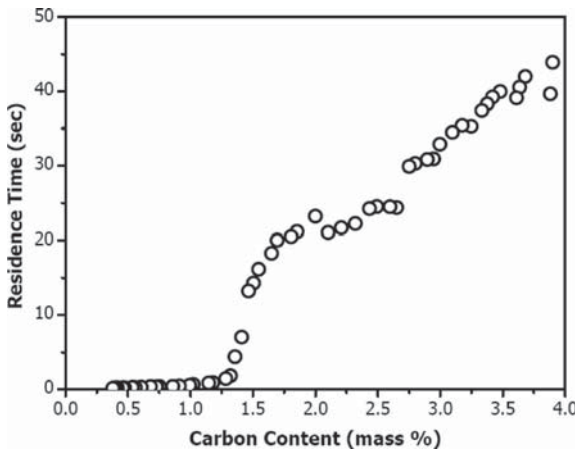

Fig. 3. Residence times of droplets as a function of initial carbon content in the metal droplets predicted by the global model.

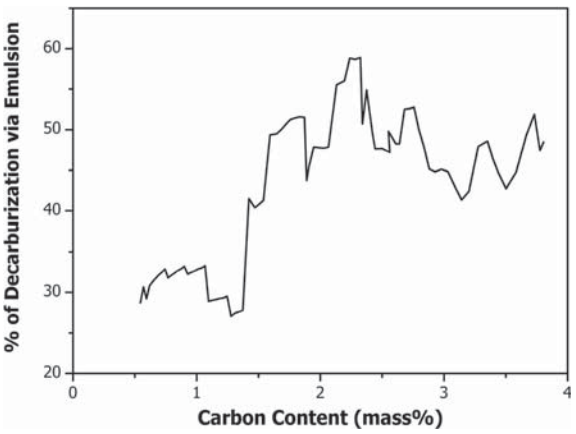

Fig. 5. Carbon removal via emulsion calculated by the model and based on the operating conditions described by Cicutti *et al*.[22]

variations away from these trends as the carbon concentration decreases, reflecting changes in blowing conditions, in particular, more droplets generated react in the emulsion due to a decrease in lance height. Therefore, the proportion of decarburization increases as the lance height decreases and then reaches to 60% during the main blow. This rate decreases to 30% significantly towards the end of the blow.

On the basis of the model, 60% of decarburization takes place in the emulsion phase during the main blow. The increase in decarburization rates was due to the increase in the number of droplets with long residence time in the emulsion phase. This finding emphasizes the importance of the bloated droplet theory in predicting the droplet behavior for better understanding of the decarburization during the entire blow. Towards the end of the blow, the impact zone rate becomes more important compared to the emulsion rate since the dense droplets do not promote the decarburization rate in the emulsion phase.

The global model was further simulated to investigate the sensitivity of the decarburization in emulsion model as a function of various droplet diameters ranging from 0.5 mm to 3 mm. The model predictions are shown in **Fig. 6**. As evidence from the plot, decarburization rates increases as the lance height decreases regardless to initial droplet diameter and the reaction rate curves follow similar trends until 7 min after the start of the blow. This is due to the fact that the decarburization rate is strong function of both the number of droplets and the droplet residence time and the combination of these two effects lowers the differences in decarburization rates in the early and middle stage of the blow.

At 8 min after the start of the blow, there is noticeable difference between the decarburization rates of metal droplets. The decarburization rates of large droplets decreases dramatically in comparison to the reaction rates of smaller ones. The decarburization rate of droplets with initial diameter of 3 mm is 75 kg/min while decarburization rate is 300 kg/min for droplets with initial diameter of 0.5 mm. The large droplets containing low carbon concentration have weak decarburization rates which in turn, have short residence time. They would return the bath zone in a short period time. This shows that decarburization rate strongly depends on the residence time of droplets. Additionally, the model suggests that maximum reaction rates in the emulsion can be achieved by the generation of smaller droplets.

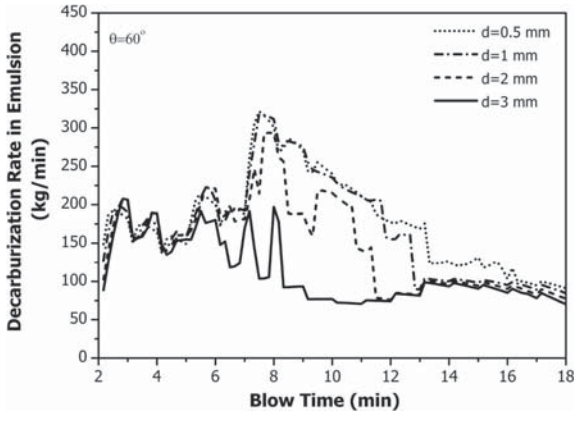

Fig. 6. Model predictions of decarburization rate in emulsion with respect to initial droplet size.

The model predictions of the carbon content of liquid iron as a function of various droplet diameters are shown in **Fig. 7**. This figure suggests that the variations in droplet size have a crucial role on the instantaneous decarburization rates of individual droplets but have a minor effect on predicting the total amount of carbon removed in the oxygen steelmaking process. This is due to the fact that total amount of carbon removed via emulsified droplets is similar regardless to the initial diameter of droplets and the mass balance calculation considers only the amount of carbon removed from the metal droplets returning to the bath as given in Eq. (1) in Part 1. For instance, the maximum difference in total amount of carbon removed was approximately 50 kg for a 10 second time step and this difference decreases to 0.5 kg towards the end of the blow.

In other words, the decarburization rates of droplets suspending in the emulsion have no influence on the overall mass balance of carbon before they return to the liquid bath. And the small variations in carbon content of liquid iron (Fig. 7) represents the periods when instantaneous decarburization rates of individual droplets has noticeable differences as given in Fig. 6 due to the differences in residence times of droplets.

3.3. Effect of Ejection Angle on Residence Time

The Droplet Residence Model was used to investigate the effects of ejection angle on droplets trajectories at various operating conditions. **Table 2** lists selected operating conditions such as variations in lance height and FeO concentrations of the slag taken from the industrial data by Cicutti *et al*. at various blowing periods to investigate the effects of different process conditions on the behavior of the metal droplets.

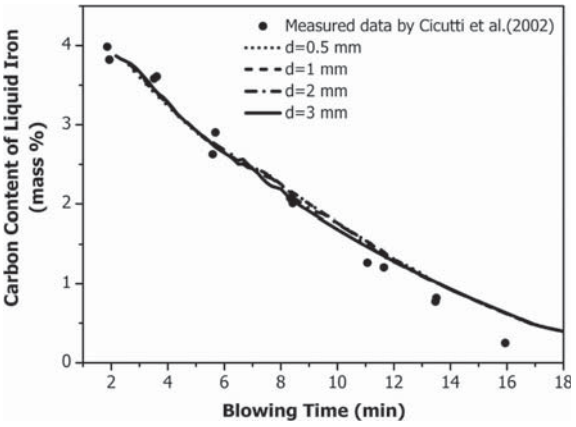

Fig. 7. Comparison of carbon content with respect to different initial drop size assumption predicted by the model.

Table 2. Measured FeO concentration and lance variations taken from the industrial data[22] at different blowing period.

	mass% FeO	Lance height	Ejection time from start of the blow	
			min	s
Early blow	31.3	2.5 m	3	00
Main blow	17.5	2.2 m	8	00
End blow	23.5	1.8 m	15	00

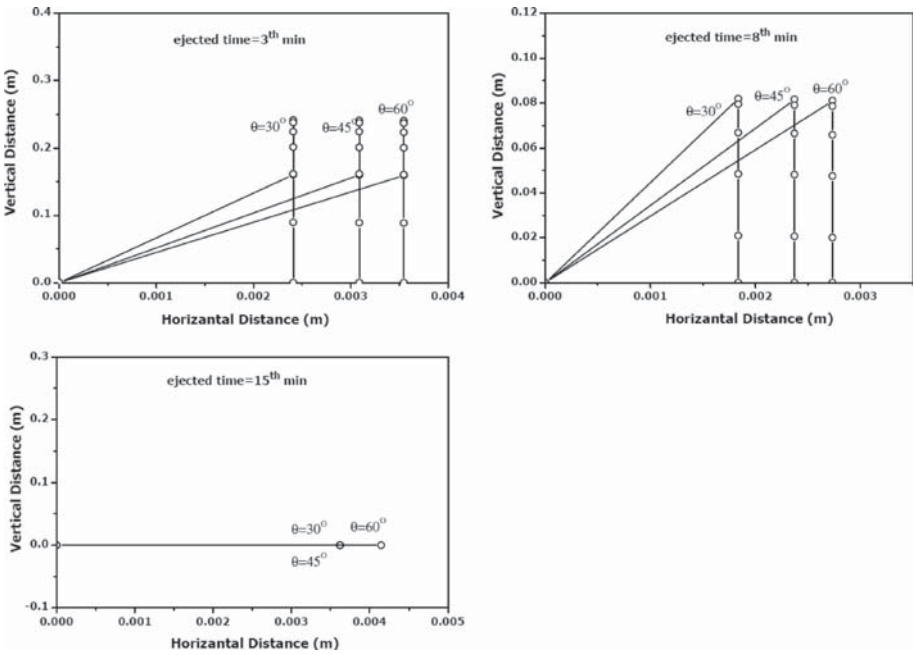

Fig. 8. Trajectories of metal droplets with different ejection angles at various blowing periods.

Figure 8 illustrates the model's predicted trajectories of metal droplets at z and r directions as a function of ejection angle. The origin point represents the ejection point of the droplets from the metal phase. This figure compares how far the droplets can travel in the emulsion phase at various ejection times given in Table 2. For instance, all the droplets ejected at 3 min. travelled 0.25 m in z direction away from the ejection point. The droplets ejected with an angle of 60° can travel the longest distance of 0.0035 m in r direction. Alternatively, the droplets ejected at 15 min. only travelled in the r direction since these droplets were dense droplets and spent short times in the emulsion phase.

Ejection angle has no influence on the vertical distance that droplets can reach for that particular blowing period. The model predicts that the metal droplets could not reach the top of the slag and the maximum height predicted varies as a function of blowing period. The highest point at z direction they are predicted is 0.25 m which is relatively short distance to the slag foam height assumed.

3.4. Effect of Ejection Angle on Decarburization Rate

The decarburization in the emulsion model was simulated for 30° and 60° ejection angle to verify this assumption. The simulations were performed for the droplets with an initial diameter of 2 mm. **Figure 9** demonstrates the change in decarburization rate predicted by the model as a function ejection angle. As seen from the figure, the decarburization curves are close to each other during the first half of the blow since the metal droplets are bloated. The model predicts that the decarburization rates using the assumption of droplet ejection in a 60 deg angle are relatively lower than those with 30 deg ejection angle. It would seem that the decarburization rate decreases as the ejection angle increases towards the end of the blow. This implies that as the droplets become dense, the ejection angle has more influence on the residence time of the droplets.

In this study, decarburization rates were calculated based on an assumption that ejection angle is constant and equals to 60° for simplicity. As discussed previously, the overall decarburization rate is expected not to be influenced by the ejection angle.

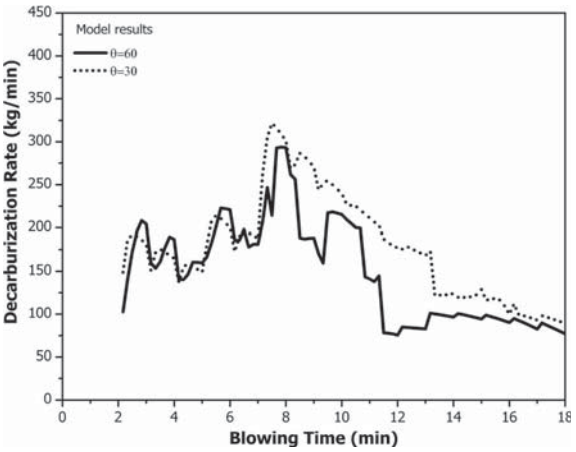

Fig. 9. Model predictions of decarburization rate with respect to ejection angle.

3.5. Carbon Content of Metal Droplets

The global model can predict the change in carbon concentration of metal droplets ejected at each time-step. **Figure 10** compares the carbon concentration of the metal droplets predicted by the global model with the measured values of carbon content of metal droplets taken from the study of Cicutti *et al*.[22] The predicted values vary in a great range due to their presence in the emulsion zone. This is due to the fact that the metal droplets may be generated, be circulating in the emulsion or be fallen back to the metal bath. Few of the results are close to those reported by Cicutti *et al*. The model predictions which are close to the measured values by Cicutti *et al*. most likely represent the carbon content of metal droplets circulating in the emulsion phase.

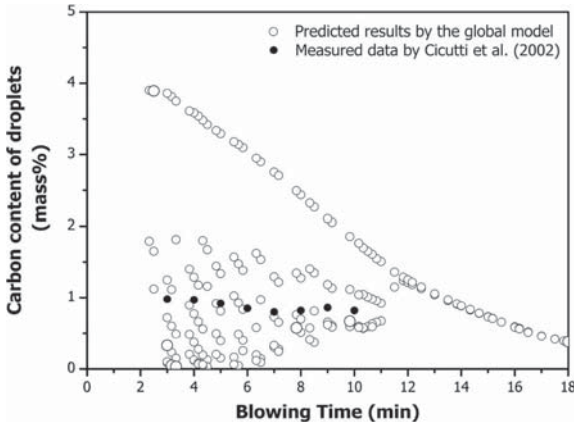

Fig. 10. Comparison of carbon content in metal droplets predicted by the proposed model with the measured carbon content of metal droplets reported by Cicutti *et al.*[22)]

However, further plant trial data is required to compare with the model.

On the basis of the model, carbon content of metal droplets freshly ejected from the bath is equal to the carbon content of liquid iron. The highest carbon concentrations for each time step represent the concentration of unreacted metal droplets. The droplets with lower concentrations represent the droplets returning to the liquid bath. The droplets with minimum carbon content have the maximum residence time in the slag-metal-gas emulsion.

As seen from the figure, there are more variations in carbon concentrations of metal droplets due to the longer residence times in the first part of the blow. Bloated droplets need more time to decarburize. On the other hand, the dense droplets suspend short times in the emulsion that they return with similar concentrations to the liquid metal.

4. Conclusion

A mathematical model has been developed to study the decarburization reaction in the slag-metal-gas emulsion for industrial practice. A numerical calculation technique was used to predict the residence time of the droplets and decarburization rates of individual droplets during the blow. This model was linked to the global model to calculate the carbon change of metal bath with time. As a result of decarburization in emulsion model, the following conclusions can be drawn.

(1) The bloated droplet theory has been applied to the industrial data. A global model including the bloated droplet theory can predict decarburization rates of individual droplets under full-scale operating conditions for oxygen steelmaking process. Decarburization rate in the emulsion zone increases as the lance height is decreased.

(2) The proposed model provides information about the variation in the residence time of the ejected metal droplets. For bloated droplets, it is predicted that the residence time of droplets in emulsion is around 45 s during the blow. Towards the end of the blow, the residence time of droplets decreases to 0.4 s.

(3) The bloated droplet theory provides sensible estimates of the decarburization rate in the emulsion zone. Ignoring the change in density would result in unrealistically low rates of decarburization and not be consistent with the plant data or the results from this study.

REFERENCES

1) E. W. Mulholland, G. S. F. Hazeldean and M. W. Davies: *J. Iron Steel Inst.*, **211** (1973), 632.
2) T. Soma and F. Tsukihashi: Proc. Int. Symp. on Physical Chemistry of Iron and Steelmaking, Canadian Institute of Mining and Metallurgy, Westmount, QC, Canada, (1982), I34.
3) C. L. Molloseau and R. J. Fruehan: *Metall. Mater. Trans. B*, **33B** (2002), 335.
4) D.-J. Min and R. J. Fruehan: *Metall. Mater. Trans. B*, **23** (1992), 29.
5) I. D. Sommerville, P. Grieveson and J. Taylor: *Ironmaking Steelmaking*, **7** (1980), 25.
6) T. Gare and G. S. F. Hazeldean: *Ironmaking Steelmaking*, **8** (1981), 169.
7) E. Chen and K. Coley: 8th Int. Conf. on Molten Slags Flux. Salts, ISS, Warrendale, PA, (2009), 803.
8) Y. Ogawa and N. Tokumitsu: Proc. of 6th Int. Iron and Steel Cong., ISIJ, Tokyo, (1990), 147.
9) B. Sarma, A. W. Cramb and R. J. Fruehan: *Metall. Mater. Trans. B*, **27** (1996), 717.
10) H. Sun: *ISIJ Int.*, **46** (2006), 1560.
11) K. Gao, V. Sahajwalla, H. Sun, C. Wheatley and R. Dry: *ISIJ Int.*, **40** (2000), 301.
12) H. Sun and G. Zhang: ICS Proc., (2005), 257.
13) E. Chen and K. Coley: *Ironmaking Steelmaking*, **37** (2010), 541.
14) L. A. Baker and R. G. Ward: *J. Iron Steel Inst.*, **205** (1967), 714.
15) L. A. Baker, N. A. Warner and A. E. Jenkins: *AIME MET SOC TRANS*, **230** (1964), 1228.
16) L. A. Baker, N. A. Warner and A. E. Jenkins: *AIME MET SOC TRANS*, **239** (1967), 857.
17) H. Sun, K. Gao, V. Sahajwalla, K. Mori and R. D. Pehlke: *ISIJ Int.*, **39** (1999), 1125.
18) G. A. Brooks, M. A. Rhamdhani, K. S. Coley, Subagyo and Y. Pan: *Metall. Mater. Trans. B*, **40** (2009), 353.
19) Subagyo, G. A. Brooks, K. S. Coley and G. A. Irons: *ISIJ Int.*, **43** (2003), 983.
20) G. A. Brooks, Y. Pan, Subagyo and K. Coley: *Metall. Mater. Trans. B*, **36** (2005), 525.
21) C. Cicutti, M. Valdez, T. Perez, R. Donayo and J. Petroni: *Latin Am. Appl. Res.*, **32** (2002), 237.
22) C. Cicutti, M. Valdez, T. Perez, J. Petroni, A. Gomez, R. Donayo and L. Ferro: 6th Int. Conf. on Molten Slags Flux Salts, ISS, Warrendale, PA, (2000), 367.
23) R. Higbie: *Trans. Am. Inst. Chem. Eng.*, **31** (1935), 365.
24) D. J. Price: in *Process Eng. Pyrometallurgy Symp.*, IMM, London, (1974), 8.
25) Subagyo and G. A. Brooks: *Can. Metall. Q.*, **44** (2005), 119.
26) R. I. L. Guthrie: Engineering in Process Metallurgy, Oxford University Press Inc., New York, (1989), 64.
27) Subagyo and G. A. Brooks: *ISIJ Int.*, **42** (2002), 1182.
28) S. C. Koria and K. W. Lange: *Metall. Mater. Trans. B*, **15B** (1984), 109.
29) E. T. Turkdogan: Fundamentals of Steelmaking, IMM, London, (1996), 138.
30) S. Ban-ya: *ISIJ Int.*, **33** (1993), 2.
31) G. K. Sigworth and J. F. Elliott: *Met. Sci.*, **3** (1974), 298.
32) K. Ito and R. J. Fruehan: *Metall. Mater. Trans. B*, **20** (1989), 515.
33) K. Ito and R. J. Fruehan: *Metall. Mater. Trans. B*, **20** (1989), 509.
34) N. Dogan, G. A. Brooks and M. A. Rhamdhani: *ISIJ Int.*, **49** (2009), 1474.
35) N. Dogan, G. A. Brooks and M. A. Rhamdhani: *ISIJ Int.*, **49** (2009), 24.